IEEE Access
Multidisciplinary | Rapid Review | Open Access Journal

Received June 14, 2020, accepted July 1, 2020, date of publication July 20, 2020, date of current version August 5, 2020.

Digital Object Identifier 10.1109/ACCESS.2020.3010339

The Spectral Optimization of a Commercializable Multi-Channel LED Panel With Circadian Impact

YI JIAU SAW[1], VINEETHA KALAVALLY[1], AND CHEE PIN TAN[2], (Senior Member, IEEE)

[1]Department of Electrical and Computer Systems Engineering, School of Engineering and Intelligent Lighting Laboratory, Monash University Malaysia, Bandar Sunway 47500, Malaysia

[2]Department of Mechatronics Engineering, School of Engineering and Advanced Engineering Platform, Monash University Malaysia, Bandar Sunway 47500, Malaysia

Corresponding author: Vineetha Kalavally (vineetha@monash.edu)

This work was supported in part by the Collaborative Research in Engineering, Science, and Technology (CREST), under Grant P20C1-15/005.

ABSTRACT There exists a need for the design of light emitting diode (LED) luminaires which can deliver both visual and non-visual benefits of light to humans. In this work, we introduce an optimization approach based on spectral shaping for a minimalistic and practical design of a circadian-tunable multi-channel luminaire which also outputs white light with high quality and luminous efficacy of radiation (LER). The spectral optimization approach utilizes Multi-objective Genetic Algorithm to maximize circadian tunability, light quality and LER while minimizing the number of channels. Solution sets are constrained using the non-visual quality metric, Melanopic Efficacy of Luminous Radiation (MELR) from the Melanopic Equivalent Daylight Illuminance (MEDI) approach and the more stringent visual quality metric TM-30 in addition to conventional Color Rendering Index (CRI). By matching theoretically optimized LED parameters to commercially available LED parameters for commercialization purposes, we establish the maximum MELR tunability that is achievable with 4 and 5 LED channels and the resulting trade-off in efficacy and light quality. Based on the results and analysis in this work, we detail a spectral optimization approach to propel the field of indoor lighting towards human-centric lighting.

INDEX TERMS Circadian lighting, human-centric lighting, indoor lighting, LED, luminaire design, melanopic equivalent daylight illuminance, multi-objective genetic algorithm, spectral optimization.

I. INTRODUCTION

In addition to light being an effective regulator of visual perception, it has now been established that it also regulates the biological clock or the circadian rhythm of humans [1]. For example, morning light is characterized by high blue content and is responsible for the onset of the biological clock in humans. Also known as the circadian clock, the biological clock which regulates the human sleep-wake cycle is an outcome of melatonin secretions in the body, directly impacted by the spectral properties of light incident on the eye over a period of time [2]. The need for a luminaire which allows for 'circadian tunability' was envisaged in 2002, when Berson *et. al.* identified a new photoreceptor, the intrinsically photosensitive retinal ganglion cells (ipRGCs) that transmit light stimuli to the suprachiasmatic nucleus (SCN) which governs the regulation of the circadian, hormonal and behavioral systems of an organism [3], [4]. It was also discovered that the ipRGCs are maximally sensitive to blue light between 446 to 477 nm [4]–[6]. This brings the possibility of artificial lighting being both beneficial and detrimental to human health. Several human circadian photo-transduction models have been proposed by Brainard *et al.* [5], Thapan *et al.* [6] and Gall *et al.* [7]. Extensive studies have shown that exposure of photo-biologically active light at inappropriate timing and intensity [8], [9] affects human health eliciting retinal damage [10], [11], glucose tolerance impairments [12]–[14] and negative impact on psychological and physiological health [13]–[15]. There are also past works on the effects of melatonin suppression due to light at night (LAN) on certain types of cancers such as breast cancer [16], colorectal cancer [17] and endometrial cancer [18] and the development of tumors [19]. On the other hand, studies have also suggested that light exposure scheduling can be implemented to treat jet-lag disorder and promote circadian entrainment in night-shift workers as a countermeasure to

The associate editor coordinating the review of this manuscript and approving it for publication was Dongxiao Yu.

circadian disruption by exposing them to temporary bright light for higher productivity and restricting bright light in the latter shift period [20], [21]. Similar approach can also be applied to re-entrain the circadian cycle of intensive care and post-operative patients in a hospital [22], for example certain healthcare facilities in Scandinavia [23], [24] and United States [25] are already implementing variable spectrum lighting. Figueiro *et. al.* also demonstrated that lighting tuned for a specific purpose such as to instigate the circadian system can reduce sleepiness and increase alertness and vitality in white-collar workers, thus increasing productivity [26]. Thus, now exists the concept of healthy lighting, which is lighting designed for optimal human health aside from one that is designed purely for visual performance.

With the emergence of multi-channel LED-based lighting systems, spectral tuning is now realizable as opposed to traditional lights with a fixed spectrum such as fluorescent lamps and single-channel white LED luminaires. Some literature on the implementation of these multi-channel luminaires are from Chew *et. al.* [27] illustrating the design of an 8-channel spectrally tunable luminaire integrated with a novel closed-loop algorithm and its capacity to replicate target spectra and Tang *et al.* [28] presenting a color control methodology for multi-channel luminaire systems using the camera on Android smartphones as the feedback sensor. The significance of a spectrally tunable luminaire is that the light's spectral power distribution (SPD) can be tuned during the course of a day such that it positively impacts the human circadian rhythm while consistently delivering high visual and energy performance. The minimalistic design of a multi-channel luminaire with tunable circadian impact has two major considerations: (1) the minimum number of LED channels to achieve a desired tunability and (2) the selection of optimal LED parameters. The optimization is usually carried out using a multi-objective optimization approach involving a metric representing circadian impact such as Circadian Action Factor (CAF) [7], Circadian Stimulus (CS) [29] or Equivalent Melanopic Lux (EML) [30], one for visual performance such as Color Rendering Index (CRI), Color Quality Scale (CQS) or TM-30 [31] and an energy efficiency metric, usually luminous efficacy of radiation (LER). In addition, the panel for maximum tunability with minimum number of LED channels must be commercially viable.

The abovementioned multi-objective optimization problem has been solved in past spectral optimization works using Steepest Descent Hill Climber Search Algorithm (SDHCS), Interior Point Algorithm (IPM), Multi-objective Genetic Algorithm (MOGA) and brute force optimization methods. The SDHCS algorithm, which is a well-known local search algorithm was used in the characterization, modelling and optimization of a 7-LED system for general illumination [32] with reliability that would worsen if the fitness landscape had multiple local minima of large widths through the search space. Due to its metaheuristics of finding local optima, it may not necessarily give the global optimum out of the search space. In addition, it is computationally intensive diminishing the practicality of the method, particularly for the case of larger numbers of LED channels [32]. On the other hand, the IPM implementation [33] in Dai *et al.* [34] aimed to maximize Circadian Action Factor (CAF) tunability and Color Rendering Index (CRI) of a mixture of dichromatic phosphor-converted blue-centered LED, dichromatic phosphor-converted green-centered LED, and a monochromatic red LED after converting the bi-objective optimization problem into single-objective functions to be minimized. IPMs are generally used to solve linear and non-linear convex optimization problems and it is applicable in this nonlinear programming problem as it allows for constrained optimization. The results for IPM however are highly dependent on the initial point which must be sufficiently distant from the boundary of the positive orthant [35]–[37]. Furthermore, the efficiency of this algorithm is strongly dependent on techniques of linear algebra which are adopted to solve the Newton equations. Additional techniques such as the predictor-corrector [37], [38] or centrality corrector technique [39], [40] may have to be implemented alongside the IPM for certain cases, increasing its complexity [41]. IPM, while unrivalled in its initial speed towards optimality, slows down when the demand for a solution that requires higher accuracy making it a liability [41]. Literature presents MOGA [42], which is an evolutionary algorithm, to be the more common multi-objective optimization approach. Genetic algorithms are global search algorithms with population-based metaheuristics, thus preserving and improving multiple potential solutions by guiding the search through population attributes. Due to its stochastic nature, the algorithm is resistant to local optima and it is also suitable for computationally complex problems with its ability to be implemented in parallel. This ability allows close to linear speedups [43]. Using MOGA techniques, Zhang *et al.* [44] attempted to minimize the blue light hazard efficiency of radiation (BLHER) while maximizing the visual performance. Bin *et al.* [45] reported the maximum CAF tunability of Quantum-dots Luminescent Mesoporous Silica-based White LEDs (QDs-WLEDs) and its dependence on the QDs' peak wavelength and Full Width Half Maximum. Abeysekera *et. al.* tackled a common design problem that exists within the subject of multi-channel luminaires which is the non-uniformity in terms of illuminance and color distribution using MOGA as well [46]. Aside from using optimization algorithms, optimization for maximum CAF variability was performed by iterating every possible SPD by brute force in [47]. This form of exhaustive search approach while is the simplest metaheuristic, it is also computationally intensive.

Regarding works related to spectral optimization, Oh *et. al.* compared the properties of commercialized artificial lighting, daylight and optimized four-package white LEDs comprising of a long-wavelength pass dichroic filter (LPDF)-capped, phosphor-converted red, amber and green LEDs (PC-LEDs) and a blue LED (R, A, G, B four-package white LEDs) [48]

and reported that most R, A, G, B four-package white LED systems had better visual performance, color quality and wider circadian impact tunability than commercialized artificial light sources [48]. Khanh *et. al.* implemented spectral optimization of an 8-LED channel luminaire for Circadian Stimulus (CS) as a measure of the non-visual impact and the chroma enhancement of red objects to quantify visual quality and it was found that it was not possible to optimize for both high CS and strong red oversaturation due to contradicting spectral sensitivity functions [49]. Dai *et al.* [50] reported that for any fixed CCT target, the luminous efficacy decreases with increasing circadian efficacy, regardless of the circadian model that is implemented when following the traditional approach of improving the spectral luminous efficacy rather than the circadian efficacy. However, the fundamental trends of the circadian efficacy variation with the luminous efficacy for both circadian models implemented show a notable deviation from each other. In a separate paper [51], Qi Dai *et. al.* demonstrated that the typical approach of optimizing light by prioritizing high visual quality may lead to ineffective circadian entrainment due to inefficient delivery of circadian activation content in light. For a target CS of 0.35, higher corneal illuminance and irradiance were necessary to achieve the target CS despite allowing higher luminous efficacy. This further reiterates the necessity of accounting for both circadian action and visual quality in spectral optimization for human-centric lighting. Optimization efforts leading to the selection of LEDs for a multi-channel luminaire are many but sporadic and none focusing on the optimum number of channels for wide circadian tunability of the luminaire as a key objective while considering the practicality of the design for commercialization, albeit being the primary reason for its slow adoption by the industry.

In this paper, we adopt the Non-dominated Sorting Algorithm II (NSGA-II) with inequality constraints proposed by Deb *et al.* [52] among MOGA techniques for spectral optimization for circadian content tunability as it is most widely applied in optimization works [53]–[55] due to its rapid non-dominated sorting approach. This approach permits relatively low computation complexity, uniform Pareto solution distribution through crowded distance estimation procedure, the elitist keeping mechanism and a straightforward crowded comparison operator [42], [56]. It is reported to outperform other evolutionary algorithms such as the Pareto Archived Evolution Strategy (PAES) [57] and Strength Pareto Evolutionary Algorithm (SPEA) [58]. The inequality constraints can also be easily adapted as it is a generic approach to introduce constraint as a penalty function [44], [59], [60].

In this work, we present a novel approach towards the minimalistic design of a multi-channel LED panel extending over the choice of LED channel numbers to practical considerations considering not only a wide circadian tunability, but also high quality, high efficacy with a practical selection of LEDs for commercialization purposes. We also implemented a figure of merit to quantify circadian action which has never been used in existing spectral optimization works. This has the potential to realize healthy circadian entrainment in humans leading to many physiological and psychological benefits. Section II presents the spectral optimization approach followed by the results and discussion of the optimization in section III. Section IV concludes the paper providing a summary of the results obtained.

II. OPTIMIZATION APPROACH FOR MULTI-CHANNEL LED PANEL WITH WIDE CIRCADIAN TUNABILITY

The optimal design of a widely circadian tunable multi-channel LED panel depends on fulfilling conflicting criteria of high quality and high luminous efficacy of radiation (LER) for the spectral design. In this section, we describe the GA approach used to solve the corresponding optimization problem.

A. OPTIMIZATION USING GA

We used a controlled elitist genetic algorithm (CEGA) which is a variant of the non-dominated sorting genetic algorithm II (NSGA-II) [52] to solve our optimization problem. The optimization routines were run using the GA toolbox under the MATLAB environment which allowed the convenient run of the CEGA. Since multi-objective optimization problems have multiple optimum solutions with the same level of merit, a set of non-dominated solutions are obtained using CEGA. As the solutions cannot be modified to improve the merit of one optimization target without degrading another, the final set of solutions of the optimization function is presented using a Pareto front [61]. The CEGA algorithm is initialized by randomly generating a collection of design variables (chromosomes) to form the starting generation. The algorithm stops optimizing when the spread between the Pareto individuals does not show a considerable change between generations. The NSGA-II determines Pareto optimal solutions, all of which are acceptable with certain trade-offs. For an n-dimensional MOP with m objective functions $f_1(x), f_2(x), f_3(x), \ldots, f_m(x)$, the aim is to find a solution vector x which satisfies the constraints and optimizes the objective functions. The solution vector is x_i where a solution x_1 is said to dominate another solution x_2 if both of the following conditions are satisfied: For all objectives, the solution x_1 is no worse than x_2, $\forall i \in \{1, m\} \rightarrow f_i(x_1) \geq f_i(x_2)$ and the solution x_1 is strictly better than x_2 in at least one objective, $\exists j \in \{1, m\} \rightarrow f_i(x_1) \geq f_i(x_2)$. The computational complexity, denoted in terms of running time of the CEGA is constrained by $O(GMN^2)$ with G representing the number of generations, M the number of objectives and N the population size [62].

In the following two sections, the metrics used to define luminous efficacy, visual quality and non-visual quality to be used in the optimization of the multi-channel LED panel are defined followed by a description of the optimization approach.

B. SPECTRAL OPTIMIZATION FOR WIDE CIRCADIAN TUNING

The Luminous Efficacy of Radiation (LER), *K (lm/W)* is used to represent the visual stimuli per unit input power. Assume the SPD of light from a multi-channel luminaire is expressed as

$$S(\lambda) = \sum_{i=1}^{n} I_i S_i(\lambda) \tag{1}$$

where $I_i \in [0, 1]$; $\lambda_i \in [380nm, 780nm]$ are the normalized intensity and peak wavelength of the LED channels, respectively. Assuming that most monochromatic LED spectra closely follow a Gaussian distribution [63], the SPD of the i^{th} channel can be expressed as

$$S_i(\lambda) = \frac{1}{\sigma\sqrt{2\pi}} e^{-\frac{1}{2}\left(\frac{\lambda-\lambda_i}{\sigma}\right)^2} \tag{2}$$

where σ is the standard deviation related to the Full Width Half Maximum (FWHM) as $\rho = 2\sigma\sqrt{2\ln 2} \approx 2.35482\sigma$. The LER *K(lm/W)* can be expressed as

$$K = K_0 \frac{\int S(\lambda)V(\lambda)d\lambda}{\int S(\lambda)d\lambda} \tag{3}$$

where $V(\lambda)$ is the photopic spectral luminous sensitivity function specified by the CIE [64] and the constant $K_0 = 683$ lm/W represents the maximum spectral luminous efficacy regarding the visual system [7], [48], [65]. As for the visual quality metric, CRI is used to represent color rendering ability of the light source despite its well reported deficiencies [31] because till date it is still the most widely adopted standard to describe light quality [34] in a commercial setting. However, TM-30-18 [66] IES method for evaluating color rendition of a source is also applied to the optimal solutions as a constraint, in order to evaluate the more stringent visual quality impacts yet to be captured by commercial standards. The whiteness of the light is measured using D_{uv}, the distance from the chromaticity coordinate of the test illuminant to the closest point on the Planckian locus on the CIE 1931 coordinates [32], [44], [67].

On evaluating non-visual performance, we adopt the action spectrum for melatonin regulation from the equivalent α-opic illuminance approach in CIE S026/E:2018 which is based on Lucas *et. al.* 2014 [3], [68]. Recent research on human circadian system [5], [6], [65], [69]–[73] have also used a similar peak of spectral sensitivity of melanopsin (the photopigment in ipRGCs) that corresponds to the peak in Lucas' action spectra model. In terms of the quantifiable circadian content, figures of merit that are more commonly discussed are the CS, CAF, EML and the more recently proposed Melanopic Equivalent Daylight Illuminance (MEDI) [9], [74] which measures the illuminance produced by radiation conforming to standard daylight (D65) that provides an equal melanopic irradiance as the test source. We use Melanopic Efficacy of Luminous Radiation (MELR) defined as the quotient of melanopic irradiance and photopic illuminance in (4) to quantify circadian content of light as specified by CIE S 026/E:2018: CIE System for Metrology of Optical Radiation for ipRGC-Influenced Responses to Light [68]. MELR ($K_{mel,v}$) allows the ease of being able to work with normalized LED intensities which can potentially be scaled to any desired lumen rating in the luminaire design process and can be expressed as

$$K_{mel,v} = \frac{\int S(\lambda)s_{mel}(\lambda)d\lambda}{K_0 \int S(\lambda)V(\lambda)d\lambda} \tag{4}$$

where $s_{mel}(\lambda)$ is the melanopic action spectra representing the normalized relative spectral sensitivity of the ipRGC photoreceptor to optical radiation incident at the cornea. It is broadly understood that exposure to high MELR lighting triggers greater activation of the human circadian system as compared to low MELR lighting.

The optimization is studied under designated constraints on the relative intensities of the light mixture and the required approximate whiteness dictated by its distance from the black body locus, $D_{uv} < 0.0054$ [44], [75]. The FWHM of the LEDs is restricted to a range between 10 to 35 nm to match typical values in commercially available LEDs. The individual differences in the red, blue, green regions are ignored at the optimization stage since matching to commercial LEDs is carried out in stage 2. To ensure an acceptable light quality, the CRI is bounded to be within 80 to 100 and luminous efficacy is constrained to be a minimum of 130 lm/W as a baseline for a commercial LED-based luminaire [76].

The aim of this multi-objective optimization problem with inequality constraints is to maximize the K and CRI to achieve the widest MELR tunability as the direct optimization goals as illustrated in the flowchart in Figure 1. The solution vector is

$$x_i\{\lambda_1^i, \lambda_2^i, \ldots, \lambda_n^i, I_1^i, I_2^i, \ldots, I_n^i, \rho_1^i, \rho_2^i, \ldots, \rho_n^i\}$$

where $\{\lambda_1^i, \lambda_2^i, \ldots, \lambda_n^i\}$, $\{I_1^i, I_2^i, \ldots, I_n^i\}$ and $\{\rho_1^i, \rho_2^i, \ldots, \rho_n^i\}$ are the peak wavelengths, normalized intensities and FWHMs for a set of n LEDs, respectively.

From the first optimization process (GA1), the optimized number of channels serve as the input in the subsequent stage of extracting commercialized LED specifications which are closest to the optimized LED parameters. It is a necessary step as the output from GA1 serve as a starting point, or a reference from which we can extract commercially available LED parameters, as there are innumerable possibilities within the visible light region, with some solutions not yet commercially existent. Having filtered the solution sets which do not satisfy the K, CRI and D_{uv} constraints, the algorithm runs through the database containing a comprehensive list of commercially available LED parameters from established brands and selects the closest match in terms of wavelength and FWHM of the channels from the optimization output. The selection algorithm compares the area under the overlapping spectra of the simulated and commercialized LED using the trapezoidal method [77] with the algorithm returning a

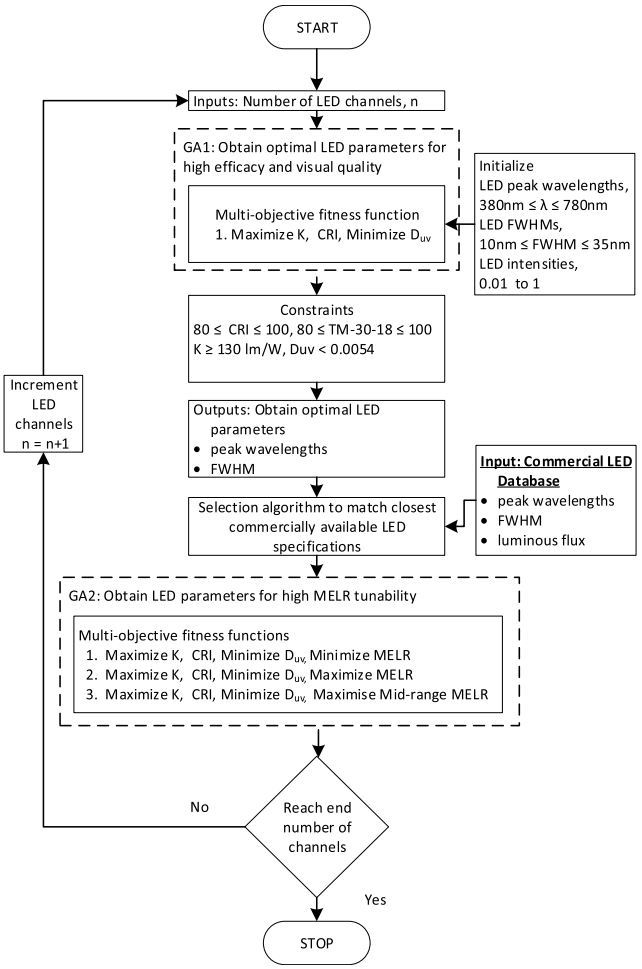

FIGURE 1. Flowchart illustrating the spectral optimization approach. This multi-objective optimization problem solves towards a practical multi-channel luminaire design with circadian tunability.

100% match if the spectra of all 4 channels match perfectly. The algorithm thus selects the best match, ensuring minimal trade-off between the theoretical and commercially available parameters. To ensure the final outputs satisfy the objective of this design approach, using the solution sets which are the parameters of commercially available LEDs from the prior stage, they become the input variables for the next stage of optimization (GA2).

In this part of the optimization, the LED peak wavelengths and FWHMs are fixed based on commercial availability, with the design variables being the channel intensities. The objective functions are the CRI, K and MELR tunability. MELR tunability can only be ascertained when the minimum and maximum MELR producible by the selected LED parameters are known. However, it is not possible to minimize and maximize the objective function simultaneously. Thus, the optimization is performed 3 times: once to determine the lowest producible MELR, another for the maximum MELR and lastly for the solutions within the range from the minimum to the maximum allowable MELR which we termed as the mid-range optimization. The purpose of the last optimization is to allow for a continuous and smooth MELR tuning within the range after prototyping. For the mid-range optimization, the algorithm uses a Gaussian distribution which emphasizes the range of MELRs that should be prioritized by the optimization, which would be the range within the specified minimum and maximum MELR.

The bounds for MELR tunability is set using spectral data of bright blue daylight at 7 a.m. and bedroom lighting measured with a CL500A Konica Minolta illuminance spectrophotometer. The MELR of bright blue daylight at CCT 10000K is at 1.8 and the MELR of bedroom lighting in the late evening at CCT 2700K is at 0.36. This range is used to define MELR tunability as the ratio of the difference between the maximum MELR and the minimum MELR achievable by the combination of LED parameters over the desired range of MELRs from bedroom lighting (MELR = 0.36) to bright blue sky (MELR = 1.8). A MELR tunability of 1 indicates perfect coverage of the required MELR range. Using MATLAB's multi-objective genetic algorithm, K and CRI were maximised while D_{uv} was minimised simultaneously for GA1. Consider the following vector:

$$\overrightarrow{F}(\overrightarrow{X}) = \left[F_1(\overrightarrow{X}), F_2(\overrightarrow{X}), F_3(\overrightarrow{X})\right] \tag{5}$$

where the objective functions are

$$F_1(\overrightarrow{X}) = -CRI, \quad F_2(\overrightarrow{X}) = -K, \; F_3(\overrightarrow{X}) = D_{uv}.$$

The multi-objective optimization problem for GA1 is posed as follows:

$$\begin{aligned} &\min \overrightarrow{F}(\overrightarrow{X}) \\ &\text{subject to constraints } F_1(\overrightarrow{X}) \le 80, \quad F_2(\overrightarrow{X}) \le 130, \\ &\qquad\qquad F_3(\overrightarrow{X}) \le 0.0054. \end{aligned} \tag{6}$$

For GA2, the algorithm was run three times with the same channel parameters and objective functions as GA1, but with one additional objective function: once to maximise MELR, once to minimise MELR and lastly to optimize within the desired middle MELR range. The optimization problem is posed as:

$$\min \overrightarrow{G}(\overrightarrow{X}) = \left[G_1(\overrightarrow{X}), G_2(\overrightarrow{X}), G_3(\overrightarrow{X}), G_{k=4,5,6}(\overrightarrow{X})\right] \tag{7}$$

where $G_k(\overrightarrow{X})$ is dependent on whether it is maximizing (k = 4) or minimizing (k = 5) the MELRs or optimizing for the solutions within the MELR range (k = 6). The objective functions for GA2 are as follows:

$$\begin{aligned} &G_1(\overrightarrow{X}) = -CRI, \quad G_2(\overrightarrow{X}) = -K, \; G_3(\overrightarrow{X}) = D_{uv} \\ &G_4(\overrightarrow{X}) = -\text{MELR}, \quad G_5(\overrightarrow{X}) = \text{MELR}, \\ &G_6(\overrightarrow{X}) = -\text{MELR}_{mid}, \end{aligned}$$

subject to constraints

$$G_1(\overrightarrow{X}) \ge 80, \quad G_2(\overrightarrow{X}) \ge 130, \; G_3(\overrightarrow{X}) \le 0.0054.$$

Once the optimization is completed for all solution sets for a specified number of channels, 3 in this case, it is incremented by 1 up to 5 channels and the optimisation process is repeated for all solution sets. Optimization terminates when all solution sets for the different number of channels are complete. The MELR tunability and other spectral characteristics are calculated and the solution sets with no valid solutions are discarded. Based on certain justifications, the number of channels and the corresponding LED parameters are chosen and the number of LEDs required per channel is computed based on the required lumen rating of the lamp using the lumens/Watt rating of LEDs from the commercial database.

III. RESULTS AND DISCUSSION

The spectral optimization procedure is performed over 50 iterations on a population of 200 chromosomes per generation. It was found that convergence occurs within 50 iterations. GA optimization halts when the optimum fitness of 2 consecutive generations is smaller than the convergence tolerance. Intermediate Crossover is used to perform crossover for functions with external constraints. It creates child chromosomes by taking weighted averages of two parent chromosomes. The weights are randomly calculated at each crossover operation. The crossover probability is intentionally set to a high value to prevent subsequent generations from having repetitive parent chromosomes which may lead to a deadlock. The Adapt Feasible Mutation function optimizes chromosomes with bounds and external constraints. It adapts with respect to previous generations depending on their success. However, the mutation probability is intentionally set to a low value to prevent the search algorithm from turning into a primitive random search. Selection functions select parent chromosomes from the current generation to initialize the next generation. Stochastic selection function selects parent chromosomes based on their fitness scores. The tournament selection function is a commonly used highly generalizable selection function. The Pareto fraction sets the amount chromosomes to be retained from the lower Pareto fronts while the solver selects individuals from higher fronts. GA parameters used for the optimization are summarized in Table 1. The population size was chosen via experimentation to ensure sufficient initial surface exploration leading to a solution that does not go into premature convergence.

The optimization process of the mixed-color white light is executed within the approach described in the previous section on an Intel® Core™ i7-7700HQ CPU 2.80 GHz with 7.89 GB memory. The mixed-color spectrum is generated by summing individual Gaussian spectra within the visible light spectrum which ranges from 380 nm to 780 nm with a resolution of 1 nm, with FWHM ranging from 10 to 35 nm and normalized intensities ranging from 0.01 to 1 [78]. The optimization process is separated into 2 stages and 1 commercial LED selection process. The optimization run time for 1 solution set is approximately 1200 seconds on average.

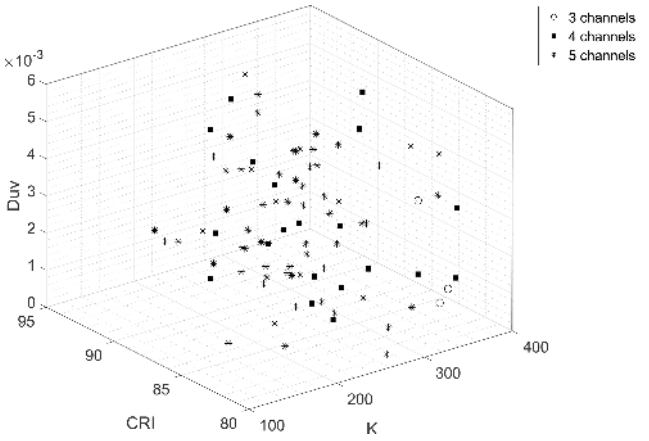

FIGURE 2. Theoretical LED combinations satisfying quality (CRI > 80) and efficacy (K > 130 lm/W) and color criteria (D_{uv} < 0.0054) for 3, 4 and 5 channels (without circadian considerations). Each point represents a unique LED combination.

TABLE 1. GA parameters used for the optimization approach.

GA Parameters	Spectral Optimization
No of chromosomes in population	10000
Maximum number of generations	200 x number of variables
Crossover function	Intermediate Crossover
Crossover probability	0.8
Mutation function	Adapt Feasible
Mutation probability	0.2
Selection function	Tournament
No of GA cycles	5
Convergence tolerance	1e-4
Pareto fraction	0.35

The objective for the first part of the spectral optimization algorithm is to optimize for high visual quality and luminous efficacy for a given number of LED channels, in this case, between 3 and 5 channels. We observe from Figure 2 that there exists 3, 19 and 60 solution sets for the 3, 4 and 5-channel combinations respectively, that satisfy the quality criteria (CRI > 80), luminous efficacy constraint (>130 lm/W) and D_{uv} < 0.0054.

From here, it is apparent that with 3 channels, there are a limited number of solution sets that satisfy the visual quality constraints, even without the circadian tunability constraint. It also illustrates how the number of satisfactory solutions increases with higher channel allowance. For 3-channel solutions, we can observe that the solution set with the highest CRI is capped at 87 while there is a sizeable concentration of 5-channel solution sets closer to 95.

Next, we illustrate the monochromatic combinations that can deliver a required MELR and investigate the consequence of applying TM-30 quality constraint in Figure 3. If the requirement from a luminaire is to deliver a specific circadian action (MELR), then examples of combinations of 3, 4 and 5

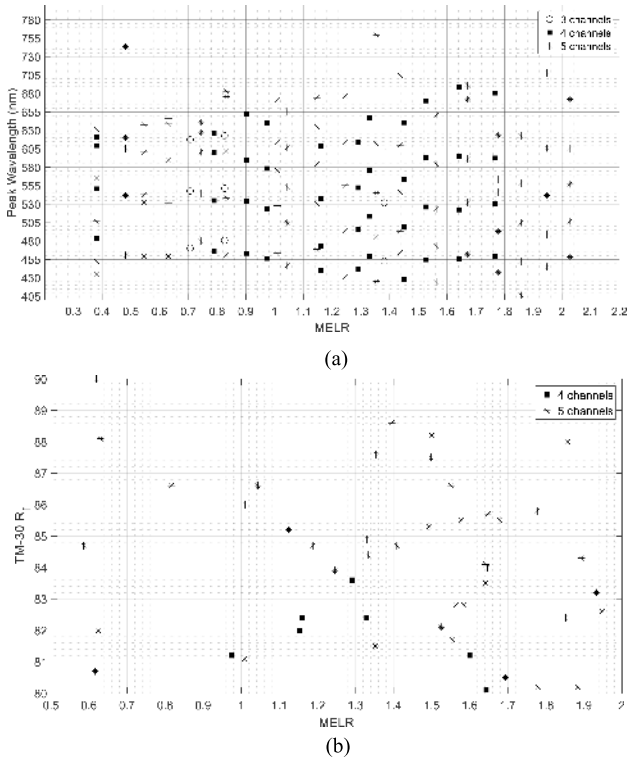

FIGURE 3. Selected LED combinations for 3, 4 and 5 channels delivering a specific MELR satisfying (a) CRI > 80, (b) CRI > 80, TM-30> 80.

channels which satisfy quality and efficacy criteria are shown in Figure 3(a). This figure depicts combinations of theoretical LED parameters, each with a certain normalized intensity (not shown in figure) which will generate white light of a specified MELR.

For example, for a 3-channel luminaire which generates a spectrum of approximately MELR 0.7, one can select LED channels with peak wavelengths at 470 nm, 547 nm and 617 nm. For a 4-channel luminaire with white light of MELR = 0.9, one can select LED channels with peak wavelengths at 463 nm, 534 nm, 590 nm and 652 nm. For a 5-channel luminaire with a spectrum of MELR = 1.95, one can select LED channels with peak wavelengths at 445 nm, 490 nm, 542 nm, 605 nm and 708 nm. With 3 channels, the maximum MELR that can be achieved is ∼1.4, with 4 channels up to ∼1.8 and with 5 channels ∼2. It is apparent that increasing the amount of LED channels correlates to the potential of achieving white light with MELR at the extremes, i.e. less than 0.8 and greater than 1.8.

From the optimization, it is evident that the solution sets satisfy the standard CRI and luminous efficacy constraints. To assure a higher standard for high quality lighting, additional filtering constraints are applied to the solution sets for the TM-30-18 visual quality criteria. The TM-30 is recently adopted by the IES and approved as the American National Standard to evaluate color rendition as it is proven to be more accurate compared to the CRI. It is a more stringent color quality evaluation metric accounting for both color fidelity and saturation, and thus, the solution sets are filtered through the TM-30-18 fidelity index $R_f > 80$ and gamut index $80 < R_g < 120$ and the results presented in Figure 3(b). There is an absence of 3-channel combinations that satisfy the TM-30-18 R_f constraint. As such, it is unnecessary to check for the R_g constraint as both must be fulfilled to satisfy the TM-30-18 criteria. Consequently, it is observed that applying the TM-30-18 constraint increases minimum channel requirement from 3 to 4, with 4 channels sufficing for MELR in the range of 0.97 to 1.64 and 5 channels from 0.58 to 1.94.

The combinations of 3 to 5 optimized LED parameters determined from GA1 serve as the input in the subsequent stage of extracting commercialized LED specifications which are most identical to the optimized LED parameters. The solution sets of the 3 to 5 optimized LED parameters are compared to a selected comprehensive database comprising the parameters of currently commercially available LEDs with a population of 64 from major LED manufacturers. The LED database comprises narrowband high-power LEDs that are typically used in commercial indoor lighting. At the time of study, there were no narrowband high-power cyan LEDs used for commercial lighting that we know of, thus there is a 50 nm gap between 550 nm and 600 nm LEDs. There also exists a gap of 46 nm between red LEDs at 675 nm and deep red LEDs at 721 nm due to the lack of red LEDs in that region, as red LEDs with wavelengths approaching the infrared region are not typically used for commercial lighting and are inefficient due to low radiant fluxes. The LED database however covers a sufficiently wide and well-distributed range within the visible light range from 447.5 nm blue to 750 nm deep red, with the widest gap of 21 nm between 634 nm red and 655 nm red with the exception of the cyan and deep red gaps. By means of the solution sets which are the parameters of commercially available LEDs from the prior stage, they become the input variables for the final part of the optimization algorithm. The selection algorithm functions to match theoretical LED parameters to commercially available LED parameters, and proceeds to optimize those parameters for wide circadian (MELR) tunability in the final stage.

In this model, the λ and ρ are pre-determined based on the outputs from the commercialized LED database. The only variables to be manipulated are the intensities of the channels. The objective functions are the CRI, K and MELR tunability which are performed in three optimization runs for minimum MELR, maximum MELR and mid-range MELR to ensure both resolution and a wide range using the same LED parameters. This model is subjected to the same constraints as in the first optimization. The solution vector in the final optimization process is $x_i = \{I_1^i, I_2^i, \ldots, I_n^i\}$ with $n = 3, 4, 5$.

A circadian-tunable luminaire requires a set of LEDs which will deliver a desired tunability. We define MELR tunability as the extent to which the range of MELRs generated by a given set of channels overlaps with a desired MELR range, $\Delta MELR$ from that of bedroom lighting min (MELR) = 0.36 (bold red line) and that of bright blue

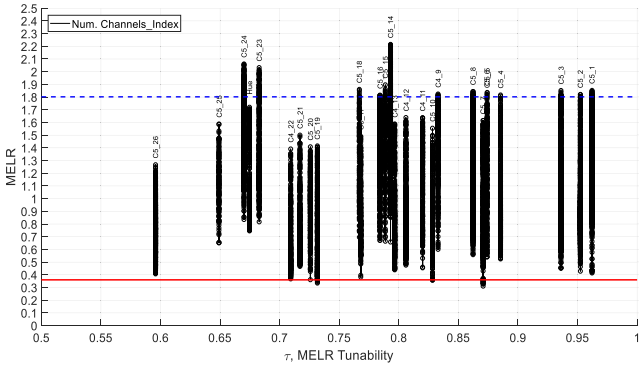

FIGURE 4. MELR tunability of 12 LED combinations with the highest MELR tunability, and the Phillips Hue overlapped with the limits of MELR tunability from that of bedroom lighting MELR 0.36 (highlighted by the bold red line) and that of bright blue daylight MELR 1.80 (highlighted by the dotted blue line).

daylight max(MELR) = 1.80 (dotted blue line) as illustrated in Figure 4. We examine the combinations that can deliver wide MELR tunability with high resolution where tunability is defined as

$$\tau = \frac{\text{MELR}_{\text{max}} - \text{MELR}_{\text{min}}}{\Delta\text{MELR}} \tag{8}$$

where $\text{MELR}_{\text{max}} \leq \max(\text{MELR})$ and $\text{MELR}_{\text{min}} \geq \min(\text{MELR})$. The MELR resolution is monitored in addition to the tunability and it is defined as the widest distance between two consecutive MELRs within a solution set. This is to ensure a gradual transition between MELRs throughout the day to avoid a drastically visible color difference between progressive light settings. In Figure 4, we also benchmarked the optimized solution sets with the tunability of the commercially available spectrally-tunable Phillips Hue bulb, by characterising its blue, green, red and neutral white LED channel spectra. The MELR tunability was found to be 0.6747, which is a relatively narrow range when compared to the solution sets that are optimized for circadian tunability.

The MELR tunability and resolution of the commercialised LED parameters are reported in descending order of MELR tunability in Table 2. The finalised selection of LED parameters for circadian lighting design is determined through two factors: high MELR tunability and resolution. Based on Table 2, combination C5_1 which is a 5-channel luminaire of peak wavelengths of 460 nm, 530 nm, 590 nm, 617 nm and 675 nm including a deep red channel gives a MELR tunability of 0.9622, whereas C5_2 with peak wavelengths [460 nm, 530 nm, 590 nm, 627 nm, 634 nm] and C5_3 with peak wavelengths [460 nm, 530 nm, 590 nm, 627 nm, 655 nm] with a smaller separation between the red and the deep red channels also allow comparable MELR tunability of 0.9524 and 0.9361 respectively.

In terms of the MELR resolution, C5_1, C5_2 and C5_3 is continuous and allow a smooth transition of the spectrum. The solution sets include peak wavelengths necessary for high quality white light with high circadian content tunability

TABLE 2. MELR tunability and MELR resolution for optimal LED combinations of 4 and 5 channels with the highest MELR tunability, and the number of LEDs per channel for each combination to produce the entire range of MELRs for 800 lumens rating. N is the total number of LEDs for the solution set.

ID	λ (nm) / ρ (nm) / I (normalised) for min MELR / I (normalised) for max MELR / Number of LEDs per channel					N	MELR Min	MELR Max	MELR Tun.	MELR Res.
C5_1	460	530	590	617	675	33	0.41	1.85	0.96	0.043
	20	30	20	20	20					
	0.024	0.067	0.155	0.078	1					
	1	0.447	0.117	0.275	0.617					
	5	5	7	3	13					
C5_2	460	530	590	627	634	21	0.43	1.82	0.95	0.029
	20	30	20	20	20					
	0.16	0.411	1	0.821	0.08					
	1	0.435	0.204	0.119	0.231					
	2	5	8	3	3					
C5_3	460	530	590	627	655	22	0.45	1.85	0.94	0.033
	20	30	20	20	20					
	0.086	0.198	0.466	0.121	1					
	1	0.444	0.157	0.277	0.236					
	2	5	7	3	5					
C4_9	460	530	590	675	-	28	0.6	1.82	0.83	0.036
	20	30	20	20	-					
	0.052	0.079	0.159	1	-					
	0.393	0.167	0.095	1	-					
	2	5	7	14	-					
C4_11	455	530	590	665	-	24	0.46	1.64	0.82	0.059
	20	30	16	20	-					
	0.046	0.105	0.311	1	-					
	1	0.454	0.377	0.946	-					
	3	5	6	10	-					
C4_12	455	530	590	634	-	20	0.48	1.64	0.81	0.028
	20	30	20	20	-					
	0.15	0.403	0.752	1	-					
	1	0.458	0.279	0.258	-					
	2	6	8	4	-					

such as 460 nm which is close to the peak of the melanopic action spectra and peak wavelengths between 500 to 600 nm which are significant for high color quality and LER [79]. All these combinations satisfy the LER constraint due to having channels close to the peak of the photopic spectral luminous sensitivity function $V(\lambda)$ of 555 nm and the color quality constraint as the spectra coincide with the peaks of the color-matching functions. These solution sets also consist of adequate long-wavelength channels to produce low MELR spectra. It is observed that LED peak wavelengths of 530 nm and 590 nm are present in most solution sets and are the key contributors to the high luminous efficacy of the spectrum.

For an SSL system with reduced complexity of only 4 channels, the 4-channel combination which allows the highest MELR tunability would be C4_9 with MELR tunability of 0.8329 and peak wavelengths [460 nm,

530 nm, 590 nm, 675 nm]. This is followed by combination C4_11 with peak wavelengths [455 nm, 530 nm, 590 nm, 665 nm] and C4_12 with peak wavelengths [455 nm, 530 nm, 590 nm, 634 nm]. For commercialization purposes, we determined the amount of LEDs required per channel based on the desired total lumens from the luminaire for the top three LED parameter combinations with the highest MELR tunability and satisfactory MELR resolution by inputting the LED parameters from the LED datasheets and the intensity ratios in order to achieve the desired MELR into the algorithm. A minimum rating of 800 lumens is employed to compute the number of LEDs required per channel, to match a typical 10-watt LED downlight that produces between 700 to 900 lumens from a standard 2.7 m ceiling height.

The results are tabulated in Table 2 as well and it is observed that although C5_1 permits the maximum MELR tunability, the overall minimum number of LEDs required for 800 lumen rating is excessive due to the low efficacy of 675nm LEDs at 6.42 lm. This increases the luminaire panel cost and design complexity. We can conclude that the optimal solution set for a 5-channel luminaire would be C5_2 with the most balanced ratio between the least number of LEDs and good MELR tunability while combination C4_12 would be the most optimal solution for a 4-channel circadian-tunable luminaire. The color coordinates of the corresponding spectra, the TM-30 color quality metric and LER tradeoff over the entire tuning range are computed and the results illustrated in Figure 5.

From Figure 5(a) and (b), the results demonstrate that the range of spectra produced by both combinations of C5_2 and C4_12 satisfy the constraint for whiteness with color coordinates close to the Planckian locus and observing and $D_{uv} < 0.0054$. Figure 5(c) and (d) depict that the generated spectra over the range of MELRs are also optimized for high visual quality as evident by the TM-30 plot of fidelity index R_f against gamut index R_g. Selecting intensity combinations which encompass the entire range of MELR producible by the solution sets, the generated spectral data are validated to satisfy the TM-30 constraints. Accordingly, the final LED parameters are undoubtedly capable of producing high quality white light spectra with the desired circadian tuning effect. It is unnecessary to validate all data points as the selected data points already comprise the conceivable MELR range. The dashed lines demarcate the approximate limits for sources on the Planckian locus while the solid lines demarcate the approximate limits for practical light sources, in which the data points fall within the region for high fidelity and good saturation range of between 80 to 120 as typical of light sources with R_f above 80. There have been no documented recommended values for the R_g as desired R_g values differ according to application of the light spectrum.

Figure 5(e) demonstrates that for both 4-channel and 5-channel luminaire designs, the efficacy is superior to the typical efficacy of a commercial white LED-based

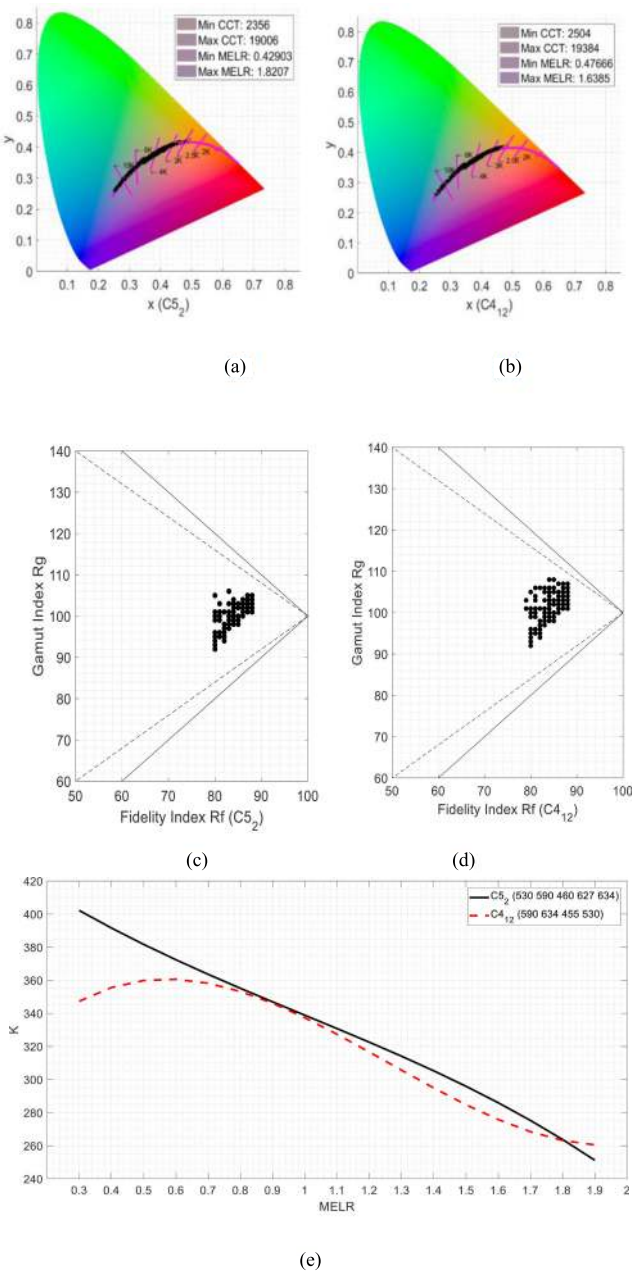

FIGURE 5. The CIE chromaticity diagram with the range of possible generated spectra by (a) C5_2 and (b) C4_12. Figure (c) and (d) illustrate that the spectra generated by C5_2 and C4_12 respectively adheres to the TM-30 criteria for high quality white light. Figure (e) plots the best-fit graphs which were extracted from the Pareto fronts and fitted to simulate the variation in efficacy with different MELRs.

luminaire of approximately 130 lm/W. This concludes that with this optimization approach, it is feasible to design for a multi-channel LED-based lighting system that is effective in promoting healthy non-visual effects of light through circadian action tunability, while delivering high visual quality and efficacy. Another observation is the non-reciprocal relationship between efficacy and MELR, which coincides with the high-luminous-efficacy optimization strategy results reported by Dai *et al.* [50]. This is by virtue of the higher

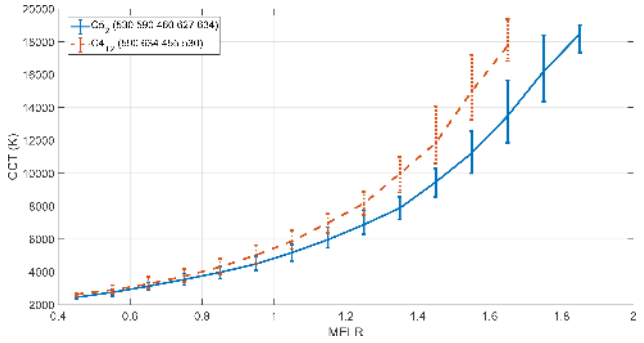

FIGURE 6. The spread of CCTs around a specific MELR for C5_2 (in blue) and C4_12 (in red dashed).

power in the blue spectral region necessary for high MELRs, which is less effective on the human photopic sensitivity function. The luminous efficacies for the 5-channel design is observed to be high for lower MELR spectra despite possessing red channels with low efficacies as a result of the 627 nm channel which compensates for the human eye insensitivity towards the longer wavelengths. Likewise, it is apparent that the 4-channel design retains lower efficacy than the 5-channel design, owing to the 5-channel luminaire having an additional red channel at that is closer to the green region, hence more effective on the human eye. Also, a more significant change in LER across MELR values is observed in the 5-channel as opposed to the 4-channel combination.

It can be deduced and has also been established that multiple spectra with the same MELR does not necessarily yield a unique CCT [80]. This can be quantified by plotting the CCT variance (across 5 spectral samples) for multiple spectra yielding the same MELR from the optimal solution set as illustrated in Figure 6. For example, a 0.65 MELR can be generated by a 4-channel spectral set with CCT ranging from 2994 K to 3689 K. At higher MELR values, a larger CCT variance of up to 4000K is observed. An inverse example is of a 12000K CCT light, which could be from spectra operating at an MELR of 1.45, 1.55 or 1.65. This further reiterates that CCT is an imperfect representation in the context of quantifying circadian content of light. Accurate evaluation of the circadian impact of light on humans can only be ascertained through actual light spectral data. It is noted from Figure 6 that the spread of CCT depends on the MELR itself with a higher spread observed at higher MELRs suggesting a higher occurrence of metameric spectra for the blue-enriched white lights.

Likewise, spectra with higher MELR feature a substantial CCT variance, which may suggest that MELR is less sensitive to the change in CCT. This can be justified as CCT calculation is dependent on how the light spectrum coincides with the three color-matching functions, however circadian content in light is only reliant on how light coincides with the melanopic action spectrum which predicts the sensitivity of the melanopsin photoreceptor.

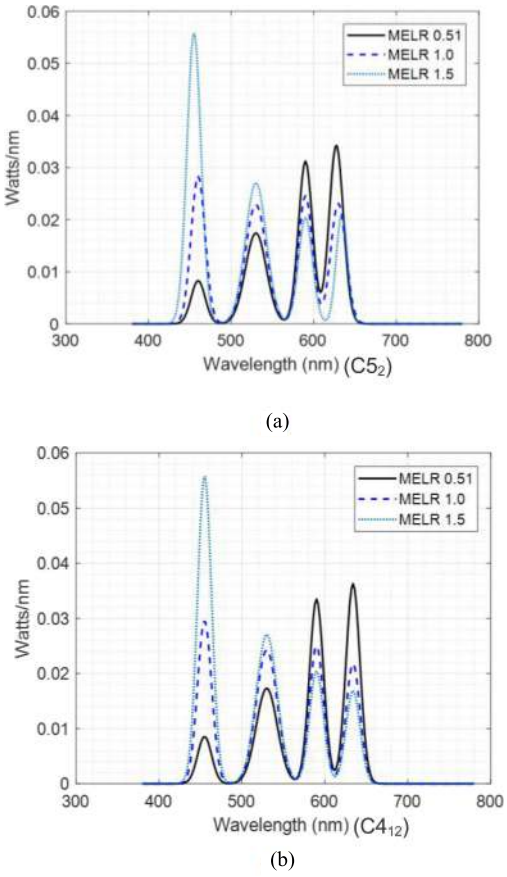

FIGURE 7. The spectral shapes with MELRs of 0.51, 1.0 and 1.5 generated by (a) C5_2 and (b) C4_12.

As the approach to the optimization is spectral shaping, spectral shapes generated by C5_2 and C4_12 for three different MELRs (0.51, 1.0 and 1.5) are delineated in Figure 7. It is clearly indicated how the spectral shape changes to generate variation in the circadian content. A higher circadian content in light quantified by a higher MELR would promote the instigation of the human circadian system, indicative of the increasing power in the blue spectral region as the MELR increases from 0.51 to 1.5.

The red spectral power exhibits dominance in the lower MELR light spectrum as shown in MELR = 0.51 producing a warmer tone of white light. For figures showing C5_2 light mixtures, only 4 peaks can be observed despite the solution having 5 channels. This is due to the superimposition of the two red channels with peak wavelengths being proximal within the visible light spectrum.

The measurements confirmed that the generated light satisfied stated light quality criteria prior to this section. *LED ColorCalculator* by OSRAM Sylvania was used to validate the results for quality as well as lumen rating.

In terms of hardware implementation and validation, the validity of the optimization results is demonstrated using a programmable light source, the Telelumen Light Replicator, which consists 16 independent visible colour channels with

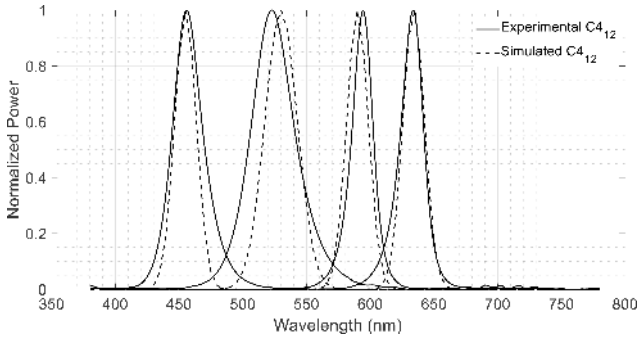

FIGURE 8. Normalized SPD plots for the optimized channels (dashed lines) and the closest experimental channels from the programmable light source (filled lines).

TABLE 3. LED channel parameters of optimized and matched 4-channel combination.

	Simulated C4_12				Telelumen (Experimental C4_12)			
λ (nm)	455	530	590	634	457	522	595	634
ρ (nm)	20	30	20	20	24	38	20	18

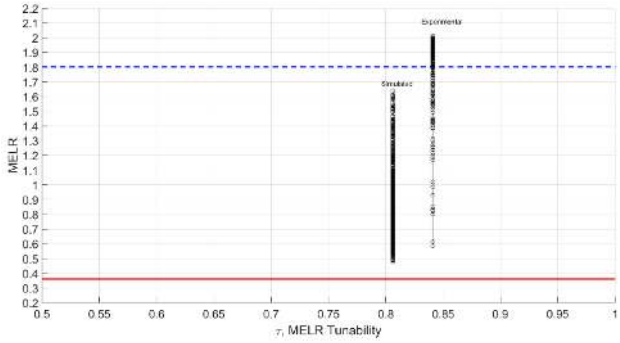

FIGURE 9. Comparison of MELR tunability achieved using optimized LED parameters and the closest available experimental LED parameters.

wavelengths ranging from 395 nm to 735 nm. The optimal combination C4_12 is selected for validation and the LED channels from the programmable light source that are most closely aligned with C4_12 as shown in Figure 8 are inputted into the optimization algorithm. Individual channel intensities for each MELR setting is determined while aiming for maximum MELR tunability. The LED parameters for the optimal combination and the corresponding hardware selection are tabulated in Table 3. Fourteen spectra are selected from the optimised results and replicated using the programmable light source inside a 1m x 1m x 1m light booth. All photometric quantities were measured using the CL-500A illuminance spectrophotometer and the MELR computed from the corresponding spectral measurements.

From a comparison between optimized and experimentally realized MELR tuning ranges shown in Figure 9, a few observations can be made. The matched LED channels

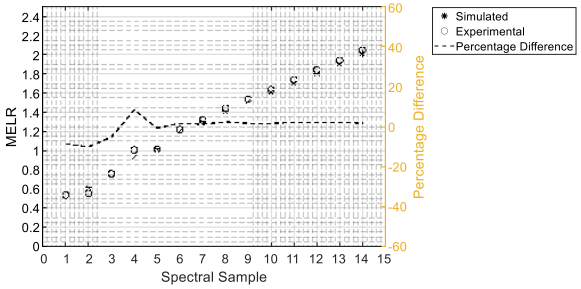

FIGURE 10. Deviation of MELR reproduction in hardware compared to simulated predictions for fourteen selected sample spectra.

from the programmable light source permit a slightly higher MELR tunability of 0.84 compared to the optimized C4_12 channels at 0.8, with the contributing factor being higher FWHM of the blue and green LED channels in the hardware set up also visible from data in Table 3. The maximum value of FWHM was constrained to 35nm in the optimisation to reflect commonly available LEDs but can be easily relaxed based on the commercial availability of LEDs if necessary. It is interesting however to note that a slight change in the LED parameters has shifted the MELR range out of the target range of 0.36 – 1.8. It has also resulted in a lower MELR resolution across the range. The hardware combination with its wider tuning range is unable to generate spectra of MELRs ranging from 0.62 to 0.8 and 1.02 to 1.17 while satisfying all the optimization constraints including visual quality. Consequently, the maximum colour difference $\Delta u'v'$ between two consecutive spectra over the entire tuning range is at 0.0331 for the experimental channels compared to only 0.0056 for optimized channels. This can impact the comfortability of the end user based on whether the perceptible color difference between MELR tuning steps is acceptable or not.

The deviation of MELR reproduction in hardware from the simulated predictions of the fourteen sample spectra generated using hardware is captured in Figure 10. The reproduction matched closely with the mean deviation of MELR and the simulated spectra at 3.54% with most reproductions within 2.5% deviation. Deviations of this scale can be expected in colour-mixed lighting systems not optimised for colour uniformity. However, a hardware realisation of our design using mature luminaire prototyping technology with spatially optimized LED placement [46] will result in a widely tunable luminaire with highly uniform illumination and color distribution.

IV. CONCLUSION

This work shows that it is feasible to design commercially realizable LED luminaires for circadian lighting that can achieve high luminous efficacy and color quality through multi-objective optimization. To date, research has mostly focused on either of the competing design objectives of lighting, i.e. visual or non-visual quality and ignore the

practicality of the design for commercialization needs. The spectral optimization of LED channels approach proposed in this study allows a wide range of circadian tunability which satisfies the non-visual design requirements of a tunable luminaire and simultaneously accounts for optimal visual quality using up-to-date metrics for both visual and non-visual quality. Metrics used to quantify the non-visual effects of light are in accordance with CIE standards and used in conjunction with the figures of merit for vision performance such as the LER, D_{uv}, CRI and TM-30.

The multi-objective optimization reveals that, for MELR tuning which satisfies the constraints of D_{uv}, CRI and TM-30, a minimum of 4 LED channels is required. The optimized 4-channel luminaire design allows an MELR tunability rating of 0.81 with MELR ranging from 0.48 to 1.64. However, as one can expect, a 5-channel luminaire is shown to permit a higher MELR tunability rating of 0.95 with MELR ranging from 0.43 to 1.82. Here, the 4-channel design can be viewed as a viable design with reduced cost and complexity while compromising insignificantly in terms of circadian tunability. Likewise, there is generally an LER trade-off observed at higher values of MELR with better LER performance perceived for 5-channel as opposed to 4-channel. However, the LER variation across the MELR values is more dramatic for 5-channel compared to 4-channels. We also found that there exists CCT variations of up to 4000K for same-MELR spectra, with larger CCT variations observed at higher MELR. Lastly, while the design in this paper was optimized for a luminaire emitting 800 lumens to satisfy standard down light lumen rating, the proposed design optimization is easily scalable to any lumen specification.

The results reported in this study are validated through the LED *ColorCalculator* simulations and using the *Telelumen Light Replicator* for hardware implementation, and the solution sets allow for the design of a minimalistic and commercializable luminaire which allows tuning for the desired circadian response. One limitation of this design approach is with the rapid turnover rate in LED models, and some becoming obsolete and new models being manufactured, they may not be included in the commercialized LED database at the time of study. Nonetheless, the approach can be used to arrive upon a new solution set as the LED database is constantly updated and expanded with the latest LED models. The optimization approach can also be applied using existing spectral data as elaborated in the experimental validation section, whereby the available color channels with their own spectral data can be optimized to satisfy the desired objectives. Lastly, the design for a given lumen rating should also be based on the actual lumen rating of LEDs which can vary between manufacturers and peak wavelengths, which will be an important consideration for PCB design and cost.

REFERENCES

[1] M. S. Rea, A. Bierman, M. G. Figueiro, and J. D. Bullough, "A new approach to understanding the impact of circadian disruption on human health," *J. Circadian Rhythms*, vol. 6, p. 7, May 2008.

[2] M. Figueiro, R. Nagare, and L. Price, "Non-visual effects of light: How to use light to promote circadian entrainment and elicit alertness," *Lighting Res. Technol.*, vol. 50, no. 1, pp. 38–62, Jan. 2018.

[3] R. J. Lucas, S. N. Peirson, D. M. Berson, T. M. Brown, H. M. Cooper, C. A. Czeisler, M. G. Figueiro, P. D. Gamlin, S. W. Lockley, J. B. O'Hagan, L. L. A. Price, I. Provencio, D. J. Skene, and G. C. Brainard, "Measuring and using light in the melanopsin age," *Trends Neurosci.*, vol. 37, no. 1, pp. 1–9, Jan. 2014.

[4] D. M. Berson, "Phototransduction by retinal ganglion cells that set the circadian clock," *Science*, vol. 295, no. 5557, pp. 1070–1073, Feb. 2002.

[5] G. C. Brainard, J. P. Hanifin, J. M. Greeson, B. Byrne, G. Glickman, E. Gerner, and M. D. Rollag, "Action spectrum for melatonin regulation in humans: Evidence for a novel circadian photoreceptor," *J. Neurosci.*, vol. 21, no. 16, pp. 6405–6412, Aug. 2001.

[6] K. Thapan, J. Arendt, and D. J. Skene, "An action spectrum for melatonin suppression: Evidence for a novel non-rod, non-cone photoreceptor system in humans," *J. Physiol.*, vol. 535, no. 1, pp. 261–267, Aug. 2001.

[7] D. Gall and K. Bieske, "Definition and measurement of circadian radiometric quantities," in *Proc. CIE Symp. Light Health, Non-Visual Effects*, Vienna, Austria: CIE, 2004, pp. 129–132.

[8] M. Hatori, C. Gronfier, R. N. Van Gelder, P. S. Bernstein, J. Carreras, S. Panda, F. Marks, D. Sliney, C. E. Hunt, T. Hirota, T. Furukawa, and K. Tsubota, "Global rise of potential health hazards caused by blue light-induced circadian disruption in modern aging societies," *npj Aging Mech. Disease*, vol. 3, no. 1, pp. 1–3, Dec. 2017.

[9] C. I. D. L'Eclairage, *Position Statement on Non-Visual Effects of Light—Recommending Proper Light at the Proper Time*, 2nd ed. Vienna, Austria: International Commission on Illumination (CIE), 2019.

[10] F. Behar-Cohen, C. Martinsons, F. Viénot, G. Zissis, A. Barlier-Salsi, J. P. Cesarini, O. Enouf, M. Garcia, S. Picaud, and D. Attia, "Light-emitting diodes (LED) for domestic lighting: Any risks for the eye?" *Prog. Retinal Eye Res.*, vol. 30, no. 4, pp. 239–257, Jul. 2011.

[11] Y. Shen, C. Xie, Y. Gu, X. Li, and J. Tong, "Illumination from light-emitting diodes (LEDs) disrupts pathological cytokines expression and activates relevant signal pathways in primary human retinal pigment epithelial cells," *Exp. Eye Res.*, vol. 145, pp. 456–467, Apr. 2016.

[12] M. G. Figueiro, L. Radetsky, B. Plitnick, and M. S. Rea, "Glucose tolerance in mice exposed to light–dark stimulus patterns mirroring dayshift and rotating shift schedules," *Sci. Rep.*, vol. 7, no. 1, p. 40661, Feb. 2017.

[13] J. H. Oh, H. Yoo, H. K. Park, and Y. R. Do, "Analysis of circadian properties and healthy levels of blue light from smartphones at night," *Sci. Rep.*, vol. 5, no. 1, p. 11325, Sep. 2015.

[14] G. Tosini, I. Ferguson, and K. Tsubota, "Effects of blue light on the circadian system and eye physiology," *Mol. Vis.*, vol. 22, pp. 61–72, Jan. 2016.

[15] H.-S. Kim and Y. H. Lee, "Correlation analysis of image reproduction and display color temperature change to prevent sleep disorder," *IEEE Access*, vol. 7, pp. 59091–59099, 2019.

[16] R. G. Stevens, G. C. Brainard, D. E. Blask, S. W. Lockley, and M. E. Motta, "Breast cancer and circadian disruption from electric lighting in the modern world," *CA, Cancer J. Clinicians*, vol. 64, no. 3, pp. 207–218, May 2014.

[17] E. S. Schernhammer, F. Laden, F. E. Speizer, W. C. Willett, D. J. Hunter, I. Kawachi, C. S. Fuchs, and G. A. Colditz, "Night-shift work and risk of colorectal cancer in the nurses' health study," *J. Nat. Cancer Inst.*, vol. 95, no. 11, pp. 825–828, Jun. 2003.

[18] A. N. Viswanathan, S. E. Hankinson, and E. S. Schernhammer, "Night shift work and the risk of endometrial cancer," *Cancer Res.*, vol. 67, no. 21, pp. 10618–10622, Nov. 2007.

[19] B. B. Otálora, J. A. Madrid, N. Alvarez, V. Vicente, and M. A. Rol, "Effects of exogenous melatonin and circadian synchronization on tumor progression in melanoma-bearing C57BL6 mice," *J. Pineal Res.*, vol. 44, no. 3, pp. 307–315, Apr. 2008.

[20] P. C. Zee and C. A. Goldstein, "Treatment of shift work disorder and jet lag," *Current Treatment Options Neurol.*, vol. 12, no. 5, pp. 396–411, Sep. 2010.

[21] K. Richter, J. Acker, S. Adam, and G. Niklewski, "Prevention of fatigue and insomnia in shift workers—A review of non-pharmacological measures," *EPMA J.*, vol. 7, no. 1, p. 16, Dec. 2016.

[22] J. D. Gleason, M. Oishi, M. Simkulet, A. Tuzikas, J. P. Hanifin, G. C. Brainard, S. R. J. Brueck, R. F. Karlicek, and L. K. Brown, "Smart lighting clinical testbed pilot study on circadian phase advancement," *IEEE J. Translational Eng. Health Med.*, vol. 7, pp. 1–10, 2019.

[23] (Feb. 7, 2018). *Ergonomic Circadian Lighting: Cases*. [Online]. Available: http://chromaviso.com/en/ergonomic-circadian-lighting/cases/
[24] A. West, P. Jennum, S. A. Simonsen, B. Sander, M. Pavlova, and H. K. Iversen, "Impact of naturalistic lighting on hospitalized stroke patients in a rehabilitation unit: Design and measurement," *Chronobiol. Int.*, vol. 34, no. 6, pp. 687–697, Jul. 2017.
[25] (Feb. 7, 2018). *Innovative Hospital Lighting System Designed to Boost Healing for Masonic Childrens Hospital Patients*. [Online]. Available: https://www.mhealth.org/blog/2016/july-2016/innovative-lighting-system-will-promote-healing-at-masonic-childrens-hospital
[26] M. Figueiro, M. Kalsher, B. Steverson, J. Heerwagen, K. Kampschroer, and M. Rea, "Circadian-effective light and its impact on alertness in office workers," *Lighting Res. Technol.*, vol. 51, no. 2, pp. 171–183, Apr. 2019.
[27] I. Chew, V. Kalavally, C. P. Tan, and J. Parkkinen, "A spectrally tunable smart LED lighting system with closed-loop control," *IEEE Sensors J.*, vol. 16, no. 11, pp. 4452–4459, Jun. 2016.
[28] S. J. W. Tang, V. Kalavally, K. Y. Ng, C. P. Tan, and J. Parkkinen, "Real-time closed-loop color control of a multi-channel luminaire using sensors onboard a mobile device," *IEEE Access*, vol. 6, pp. 54751–54759, 2018.
[29] M. S. Rea and M. G. Figueiro, "Light as a circadian stimulus for architectural lighting," *Lighting Res. Technol.*, vol. 50, no. 4, pp. 497–510, 2016.
[30] *WELL Building Standard*, Int. WELL Building Inst., New York, NY, USA, 2014.
[31] W. Davis and Y. Ohno, "Color quality scale," *Opt. Eng.*, vol. 49, no. 3, 2010, Art. no. 033602.
[32] A. Thorseth, "Optimization of light quality from color mixing light-emitting diode systems for general lighting," *Proc. SPIE*, vol. 8278, Feb. 2012, Art. no. 82781O.
[33] L. Liu and L. Fan, "The complexity analysis of an efficient interior-point algorithm for linear optimization," in *Proc. 3rd Int. Joint Conf. Comput. Sci. Optim.*, vol. 2, 2010, pp. 21–24.
[34] Q. Dai, Q. Shan, H. Lam, L. Hao, Y. Lin, and Z. Cui, "Circadian-effect engineering of solid-state lighting spectra for beneficial and tunable lighting," *Opt. Express*, vol. 24, no. 18, pp. 20049–20059, Sep. 2016.
[35] E. D. Andersen, J. Gondzio, C. Meszaros, and X. Xu, "Implementation of Interior Point Methods for Large Scale Linear Programming," Ecole des Hautes Etudes Commerciales, Universite de Geneve, Geneva, Switzerland, Tech. Rep. 96.3, 1996.
[36] E. M. Gertz and S. J. Wright, "Object-oriented software for quadratic programming," *ACM Trans. Math. Softw.*, vol. 29, no. 1, pp. 58–81, Mar. 2003.
[37] S. Mehrotra, "On the implementation of a primal-dual interior point method," *SIAM J. Optim.*, vol. 2, no. 4, pp. 575–601, 1992.
[38] I. J. Lustig, R. E. Marsten, and D. F. Shanno, "On implementing Mehrotra's predictor–corrector interior-point method for linear programming," *SIAM J. Optim.*, vol. 2, no. 3, pp. 435–449, Aug. 1992.
[39] J. Gondzio, "Multiple centrality corrections in a primal–dual method for linear programming," *Comput. Optim. Appl.*, vol. 995, pp. 137–156, Nov. 1995.
[40] M. Colombo and J. Gondzio, "Further development of mutiple centrality correctors for interior point methods," Univ. Edinburgh, Edinburgh, Scotland, Tech. Rep. 41, Sep. 2006.
[41] J. Gondzio, "Interior point methods 25 years later," *Eur. J. Oper. Res.*, vol. 218, pp. 587–601, May 2012.
[42] Y. Cui, Z. Geng, Q. Zhu, and Y. Han, "Review: Multi-objective optimization methods and application in energy saving," *Energy*, vol. 125, pp. 681–704, Apr. 2017.
[43] G. A. Gazonas, D. S. Weile, R. Wildman, and A. Mohan, "Genetic algorithm optimization of phononic bandgap structures," *Int. J. Solids Struct.*, vol. 43, nos. 18–19, pp. 5851–5866, Sep. 2006.
[44] J. Zhang, W. Guo, B. Xie, X. Yu, X. Luo, T. Zhang, Z. Yu, H. Wang, and X. Jin, "Blue light hazard optimization for white light-emitting diode sources with high luminous efficacy of radiation and high color rendering index," *Opt. Laser Technol.*, vol. 94, pp. 193–198, Sep. 2017.
[45] B. Xie, J. Zhang, W. Chen, J. Hao, Y. Cheng, R. Hu, D. Wu, K. Wang, and X. Luo, "Realization of wide circadian variability by quantum dots-luminescent mesoporous silica-based white light-emitting diodes," *Nanotechnology*, vol. 28, no. 42, Oct. 2017, Art. no. 425204.
[46] S. K. Abeysekera, V. Kalavally, M. Ooi, and Y. C. Kuang, "Impact of circadian tuning on the illuminance and color uniformity of a multichannel luminaire with spatially optimized LED placement," *Opt. Express*, vol. 28, no. 1, pp. 130–145, Jan. 2020.
[47] A. ukauskas and R. Vaicekauskas, "Tunability of the circadian action of tetrachromatic solid-state light sources," *Appl. Phys. Lett.*, vol. 106, no. 4, Jan. 2015, Art. no. 041107.
[48] J. Hye Oh, S. Ji Yang, and Y. Rag Do, "Healthy, natural, efficient and tunable lighting: Four-package white LEDs for optimizing the circadian effect, color quality and vision performance," *Light, Sci. Appl.*, vol. 3, no. 2, p. e141, Feb. 2014.
[49] T. Q. Khanh, P. Bodrogi, and T. Q. Vinh, "Human centric lighting and color quality," in *Color Quality of Semiconductor and Conventional Light Sources*. Weinheim, Germany: Wiley-VCH Verlag GmbH & Co. KGaA, 2017.
[50] Q. Dai, Y. Huang, L. Hao, Y. Lin, and K. Chen, "Spatial and spectral illumination design for energy-efficient circadian lighting," *Building Environ.*, vol. 146, pp. 216–225, Dec. 2018.
[51] Q. Dai, W. Cai, L. Hao, W. Shi, and Z. Wang, "Spectral optimisation and a novel lighting-design space based on circadian stimulus," *Lighting Res. Technol.*, vol. 50, no. 8, pp. 1198–1211, Dec. 2018.
[52] K. Deb, A. Pratap, S. Agarwal, and T. Meyarivan, "A fast and elitist multiobjective genetic algorithm: NSGA-II," *IEEE Trans. Evol. Comput.*, vol. 6, no. 2, pp. 182–197, Apr. 2002.
[53] K. Mitra, "Multiobjective optimization of an industrial grinding operation under uncertainty," *Chem. Eng. Sci.*, vol. 64, no. 23, pp. 5043–5056, Dec. 2009.
[54] J. Chen, "Multi-objective optimization of cutting parameters with improved NSGA-II," in *Proc. Int. Conf. Manage. Service Sci.*, Sep. 2009, pp. 1–4.
[55] S. P. Kodali, R. Kudikala, and D. Kalyanmoy, "Multi-objective optimization of surface grinding process using NSGA II," in *Proc. 1st Int. Conf. Emerg. Trends Eng. Technol.*, 2008, pp. 763–767.
[56] Y. Yusoff, M. S. Ngadiman, and A. M. Zain, "Overview of NSGA-II for optimizing machining process parameters," *Procedia Eng.*, vol. 15, pp. 3978–3983, Jan. 2011.
[57] J. Knowles and D. Corne, "The Pareto archived evolution strategy: A new baseline algorithm for Pareto multiobjective optimisation," in *Proc. Congr. Evol. Comput.-CEC*, vol. 1, 1999, pp. 98–105.
[58] E. Zitzler and L. Thiele, "An evolutionary algorithm for multiobjective optimization: The strength Pareto approach," Comput. Eng. Netw. Lab. (TIK), Swiss Federal Inst. Technol. Zürich (ETH), Zürich, Switzerland, Tech. Rep. 43, 1998.
[59] J. Zhang, R. Hu, B. Xie, X. Yu, X. Luo, Z. Yu, L. Zhang, H. Wang, and X. Jin, "Energy-saving light source spectrum optimization by considering Object's reflectance," *IEEE Photon. J.*, vol. 9, no. 2, pp. 1–11, Apr. 2017.
[60] K. Deb, "An efficient constraint handling method for genetic algorithms," *Comput. Methods Appl. Mech. Eng.*, vol. 186, nos. 2–4, pp. 311–338, Jun. 2000.
[61] Y. Censor, "Pareto optimality in multiobjective problems," *Appl. Math. Optim.*, vol. 4, no. 1, pp. 41–59, Mar. 1977.
[62] M. T. Jensen, "Reducing the run-time complexity of multiobjective EAs: The NSGA-II and other algorithms," *IEEE Trans. Evol. Comput.*, vol. 7, no. 5, pp. 503–515, Oct. 2003.
[63] J. Sun and J. W. Zhang, "Design of LED light source for uniform illumination in large area," *Appl. Mech. Mater.*, vols. 401–403, pp. 465–468, Sep. 2013.
[64] G. Wyszecki and W. S. Stiles, *Color Science: Concepts and Methods, Quantitative Data and Formulae*. 2nd ed. New York, NY, USA: Wiley, 1982.
[65] A. ukauskas, R. Vaicekauskas, and P. Vitta, "Optimization of solid-state lamps for photobiologically friendly mesopic lighting," *Appl. Opt.*, vol. 51, no. 35, pp. 8423–8432, 2012/12/10 2012.
[66] *Evaluating Color Rendition Using IES TM-30-15*, U.S. Dept. Energy, Washington, DC, USA, 2015.
[67] Y. Ohno, "Practical use and calculation of CCT and Duv," *LEUKOS*, vol. 10, no. 1, pp. 47–55, Jan. 2014.
[68] *CIE System for Metrology of Optical Radiation for ipRGC-Influenced Responses to Light*, Standard CIE S 026/E:2018, Commission Internationale de L'Eclairage, Vienna, Austria, 2018.
[69] S.-S. Yan and W. Wang, "The effect of lens aging and cataract surgery on circadian rhythm," *Int. J. Ophthalmol.*, vol. 9, no. 7, pp. 1066–1074, 2016.
[70] J. S. Emens and H. J. Burgess, "Effect of light and melatonin and other melatonin receptor agonists on human circadian physiology," *Sleep Med. Clinics*, vol. 10, no. 4, pp. 435–453, Dec. 2015.

[71] R. G. Stevens and Y. Zhu, "Electric light, particularly at night, disrupts human circadian rhythmicity: Is that a problem?" *Phil. Trans. Roy. Soc. B, Biol. Sci.*, vol. 370, no. 1667, May 2015, Art. no. 20140120.
[72] H. J. Bailes and R. J. Lucas, "Human melanopsin forms a pigment maximally sensitive to blue light ($\lambda_{max} \approx 479$ nm) supporting activation of $G_{q/11}$ and $G_{i/o}$ signalling cascades," *Proc. Roy. Soc. B, Biol. Sci.*, vol. 280, no. 1759, May 2013, Art. no. 20122987.
[73] R. Lasauskaite and C. Cajochen, "Influence of lighting color temperature on effort-related cardiac response," *Biol. Psychol.*, vol. 132, pp. 64–70, Feb. 2018.
[74] L. Price and L. Schlangen, *Equivalent Daylight D65 Illuminance Toolbox*, v1.05X ed. Vienna, Austria: International Commision on Illumination, 2018.
[75] J. H. Oh, Y. J. Eo, S. J. Yang, and Y. R. Do, "High-Color-Quality multipackage phosphor-converted LEDs for yellow photolithography room lamp," *IEEE Photon. J.*, vol. 7, no. 2, pp. 1–8, Apr. 2015.
[76] *CALiPER: Snapshot Industrial Luminaires*, BT Office, Energy Efficiency Renew. Energy, U.S. Dept. Energy, Washington, DC, USA, 2017.
[77] M. M. Tai, "A mathematical model for the determination of total area under glucose tolerance and other metabolic curves," *Diabetes Care*, vol. 17, no. 2, pp. 152–154, Feb. 1994.
[78] A. ukauskas, R. Vaicekauskas, F. Ivanauskas, R. Gaska, and M. S. Shur, "Optimization of white polychromatic semiconductor lamps," *Appl. Phys. Lett.*, vol. 80, no. 2, pp. 234–236, Jan. 2002.
[79] L.-L. Zheng, T.-Z. Wu, Y.-J. Lu, Y.-L. Gao, Y.-J. Wang, L.-H. Zhu, Z.-Q. Guo, and Z. Chen, "Spectral optimization of three-primary LEDs by considering the circadian action factor," *IEEE Photon. J.*, vol. 8, no. 6, pp. 1–9, Dec. 2016.
[80] L. Tähkämö, T. Partonen, and A.-K. Pesonen, "Systematic review of light exposure impact on human circadian rhythm," *Chronobiol. Int.*, vol. 36, no. 2, pp. 151–170, Feb. 2019.

YI JIAU SAW was born in Malaysia, in 1993. She received the B.Eng. degree (Hons.) in electrical engineering and computer systems from Monash University, in 2017, where she is currently pursuing the Ph.D. degree. She is also attached to the Intelligent Lighting Laboratory. Her research interests include circadian lighting from psychological, physiological viewpoints and the mathematical optimization for the design of circadian lighting.

VINEETHA KALAVALLY received the Ph.D. degree from Monash University, Australia, in 2012. She is currently an Associate Professor with the Department of Electrical and Computer Systems Engineering, School of Engineering, Monash University Malaysia, where she leads the Intelligent Lighting Laboratory. Her research interests include diverse applications of solid-state lighting, visual and non-visual quality of light, wearable light sensors, and visible light communication.

CHEE PIN TAN (Senior Member, IEEE) received the B.Eng. (Hons.) and Ph.D. degrees from Leicester University, Leicester, U.K., in 1998 and 2002, respectively. He was a Lecturer with the School of Engineering, Monash University Malaysia, in 2002, where he was subsequently promoted to a Senior Lecturer, in 2008, and an Associate Professor, in 2013. He has authored over 50 internationally peer-reviewed research articles, including a book on fault reconstruction. His research interests include robust fault estimation and observers.